Supplemental Experimental Methods.

Tissue sources

Recruitment occurred at four sites: INER-CIENI in Mexico City, Mexico (peripheral blood and cervical LN); Case Western Reserve University in Cleveland, Ohio (mesenteric LN); the University of Pennsylvania CFAR Human Immunology Core Facility (peripheral blood); and the Pathology Department, University General Hospital of Heraklion, Crete, Greece (mesenteric LN).

Cells and tissues

Peripheral blood mononuclear cells (PBMC) were purified from whole blood or leukapheresis products by Ficoll-Hypaque density gradient centrifugation. Lymph node mononuclear cells (LNMC) were isolated by mechanical disruption, performed either manually or using a gentleMACS tissue dissociator (C tubes, program h_tumor_01_01, Miltenyi Biotec). PBMC and LNMC were cryopreserved and stored at -140°C. All cryopreserved cells were thawed and rested overnight in complete medium (RPMI-1640, 10% heat-inactivated fetal bovine serum, 1% penicillin, 1% μg/ml streptomycin, and 1% L-glutamine) prior to immunostaining or stimulation. Whole LN tissue samples were fixed in formalin and paraffin-embedded prior to sectioning.

Antibodies and MHC tetramers

The following antibodies were used for flow cytometry: (1) pre-stain antibodies: α-CCR7 BV711 (clone G043H7, BioLegend), α-CCR7 APC-eFluor780 (clone 3D12, eBioscience), and α-CCR7 APC-Cy7 (clone G043H7, BioLegend); (2) surface stain antibodies: α-CD14 PE-Cy5 (clone 61D3, Abcam), α-CD14 APC-Cy7 (clone MφP9, BD Biosciences), α-CD14 BV510 (clone M5E2, BioLegend), α-CD16 PE-Cy5 or APC-Cy7 (clone 3G8, BioLegend or BD Biosciences, respectively), α-CD19 PE-Cy5, BV510 or BV785 (clone HIB19, BioLegend), α-CD4 PE-Cy5.5 (clone S3.5, Invitrogen), α-CD8a BV570, BV605 or BV650 (clone RPA-T8, BioLegend), α-CD8 QD605 (clone 3B5, Invitrogen), α-CD27 BV650 or BV785 (clone O323, BioLegend), α-CD27 QD655 (clone CLB-27/1, Invitrogen), α-CD45RO ECD (clone UCHL1, Beckman Coulter), α-CD45RO PE-BV650 (clone UCHL1, BD Biosciences), α-CXCR5 AlexaFluor488 (clone RF8B2, BD Biosciences), α-CXCR5 PE-Cy7 (clone J252D4, BioLegend), α-PD-1 APC-Cy7 or BV785 (clone EH12.2H7, BioLegend), and α-CXCR3 BV711 (clone G025H7, BioLegend); (3) intracellular stain antibodies: α-CD3 BV570 or BV711 (clone UCHT1, BioLegend), α-IFNγ AlexaFluor700 (clone B27, Invitrogen), α-TNF PE-Cy7 (clone MAb11, BD Biosciences), α-perforin BV421 (clone B-D48, BioLegend), α-perforin PE-Cy7 (clone dG9, eBioscience), α-granzyme B AlexaFluor700 (clone GB11, BD Biosciences), α-T-bet PE (clone 4B10, eBioscience), α-T-bet PE-Dazzle 594 (clone 4B10, BioLegend), α-eomes eFluor660 or AlexaFluor647 (clone WD1928, eBioscience), α-CD69 PE-Cy5 (clone FN50, BD Biosciences), and α-Ki67 FITC (clone B56, BD Biosciences).

MHC-class I tetramers conjugated to PE or BV421 were used to detect $CD8^+$ T-cells specific for SLYNTVATL (SL9)/HLA-A*0201, ILKEPVHGV (IV9)/HLA-A*0201, FLGKIWPSHK (FK10)/HLA-A*0201, RYPLTFGW (RW8)/HLA-A*2402, KYKLKHIVW (KW9) HLA-A*2402, GPGHKARVL (GL9)/HLA-B*0702, HPRVSSEVHI (HI10)/HLA-B*0702, and SPAIFQSSFM (SM10)/HLA-B*0702.

The following antibodies and reagents were used for immunohistochemistry studies: Directly conjugated α-CD20 eFluor615 (clone L26, eBiosciences) and α-perforin AlexaFluor647 (clone dG9, BioLegend) antibodies were used in combination with non-conjugated α-granzyme B (clone GrB-7, Dako) and α-CD8 (clone 4B11, Thermo Scientific). GzmB was visualized with α-mouse IgG2a AlexaFluor488 (Life Technologies), and CD8 was visualized with α-mouse IgG2b AlexaFluor546 (Life Technologies). JoJo-1 (Invitrogen), which binds nucleic acids, was used for nuclear staining.

Redirected killing assay

PBMC and Tonsil cells were thawed and rested overnight. Next day, effector cells (CD8+ T cells) were purified using a CD8+ T cell enrichment (negative selection) kit (Stemcell) for both tonsil cells and PBMCs. Tonsil cells went through further positive and negative isolation of CXCR5+/- cells using column separation (Miltenyi). The different CD8+ T cell populations were then rested for 2 hr at 37C.

Target (P815) cells were split 2 times and stained in PBS for cell tracing with TFL4 (1:3000, OncoImmunin) and detection of dead cells with LIVE/DEAD ViVid (1:2000, Invitrogen) prior to killing assay for 15 min at 37C. P815 cells were washed two times with PBS and incubated with a-CD3 (BioRad) for 30 min in dark. Target cells by themselves, or effector and target cells were co-cultured at a 1:1, 5:1 and 1:10 ratio, quickly spun down for 30 secs to pack cells, and co-incubated for 4hr at 37C in complete R10 media. Cells were then perm/fixed (BD Biosciences) and stained with active-caspase 3 FITC (BD Biosciences). Cell were then fixed and run a LSR II. Background was reduced by using LIVE/DEAD ViVid to gate out cells dead by the start of the assay. To correct for spontaneous apoptosis, all effector:target ratio killing replicates were background subtracted based on the frequency of caspase-3+ target cells in the wells with only target cells. To detect the level of redirected killing of target cells, cells were gated the following way: single cells-LIVE P815 cells-caspase-3+ (level of killing after background subtraction).

TGF-b/IL-12 induction of CXCR5 expression

Proliferation assays, as described in Materials and Methods, were performed with tonsillar mononuclear cells (n=3) labelled with CellTrace CFSE (Molecular Probes, Invitrogen). Cells were stimulated with 1µg/ml SEB (Sigma) for 5 days in the presence of plate-bound anti-CD28/CD49d (BD Biosciences) and recombinant human TGF-b1 (5ng/ml, R&D Systems) and/or IL-12 (1ng/ml, R&D Systems).

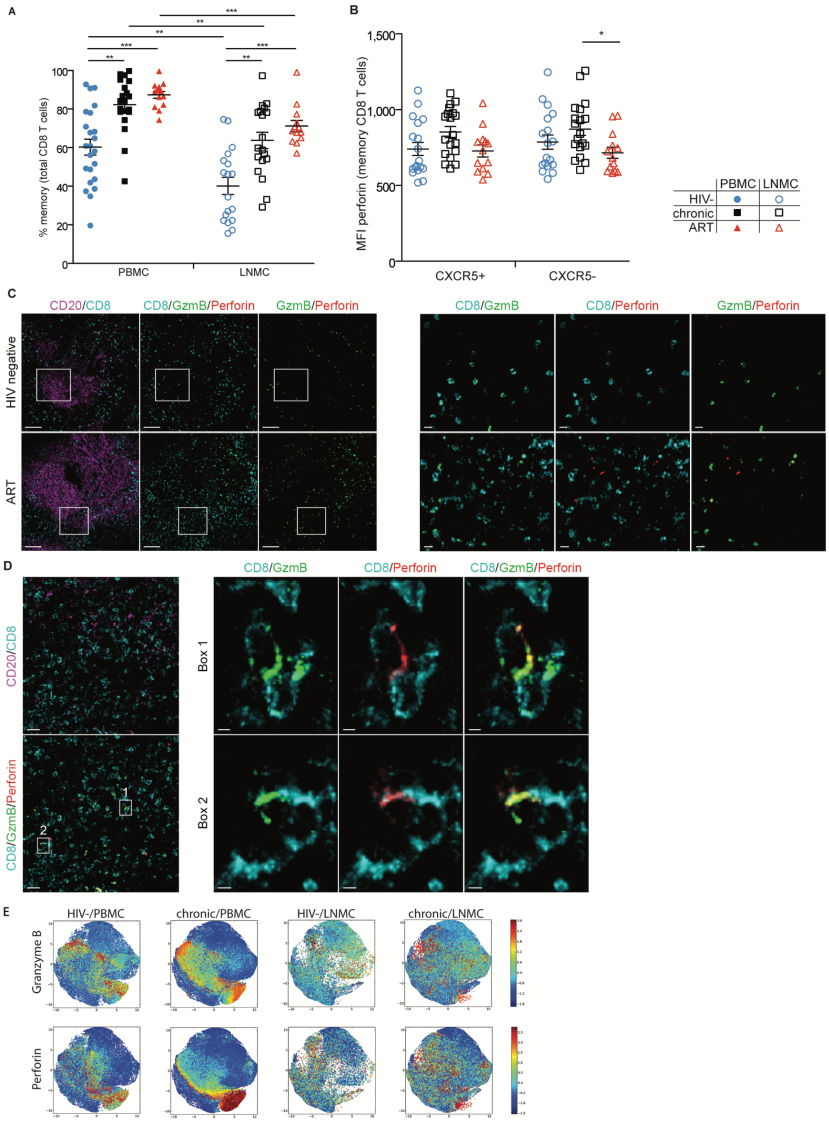

Figure S1. Memory phenotype and perforin/gzmB expression patterns in follicular and extrafollicular CD8$^+$ T-cells. Relate to Figures 1 and 2. **(A)** Memory phenotype analysis of CD8$^+$ T-cells in PBMC and LNMC based on CD27 and CD45RO expression patterns. Data shown represent cells that do not express a naïve phenotype (CD27$^+$ CD45RO$^-$). HIV$^-$ (●, ○), HIV$^+$ therapy-naïve (■, □), HIV$^+$ on ART (▲, △). **(B)** Perforin MFI in CXCR5$^+$ and CXCR5$^-$ memory CD8$^+$ T-cells in LNMC. Statistical significance between subject groups within a memory subset was determined by using the Kruskal-Wallis test with Dunn's post-test. Statistical significance within a subject group between memory subsets was determined by using the Mann-Whitney two-tailed test. For both tests: * = $P <$ 0.05; ** = $P < 0.01$; *** = $P < 0.001$. Ranges shown on plots represent mean +/- SEM. HIV$^-$ (●, ○), HIV$^+$ therapy-naïve (■, □), HIV$^+$ on ART (▲, △). **(C)** Immunohistochemistry staining of paraffin-embedded tissue sections showing CD8$^+$ T-cells within B-cell follicles. Top row: low magnification view of a representative B-cell follicle from an HIV$^-$ individual (scale bar = 100 μm). Boxes highlights areas for 10x zoom in right images (scale bar = 10 μm). Bottom row: corresponding data from an ART-treated HIV$^+$ individual. **(D)** Immunohistochemistry staining of a paraffin-embedded tissue section showing a representative image of perforin and gzmB expression in CD8$^+$ T-cells at the border between the T-cell zone and a B-cell follicle from an HIV$^+$ subject on ART. Left: scale bar = 20 μm. Boxes 1 and 2 indicate areas for 10x zoom in right images (scale bar = 200 μm). (E) Cell ACCENSE tSNE plots of perforin and gzmB expression in memory CD8$^+$ T-cells comparing PBMC vs. LNMC from HIV$^-$ and untreated HIV$^+$ individuals (based on *n*=4/group).

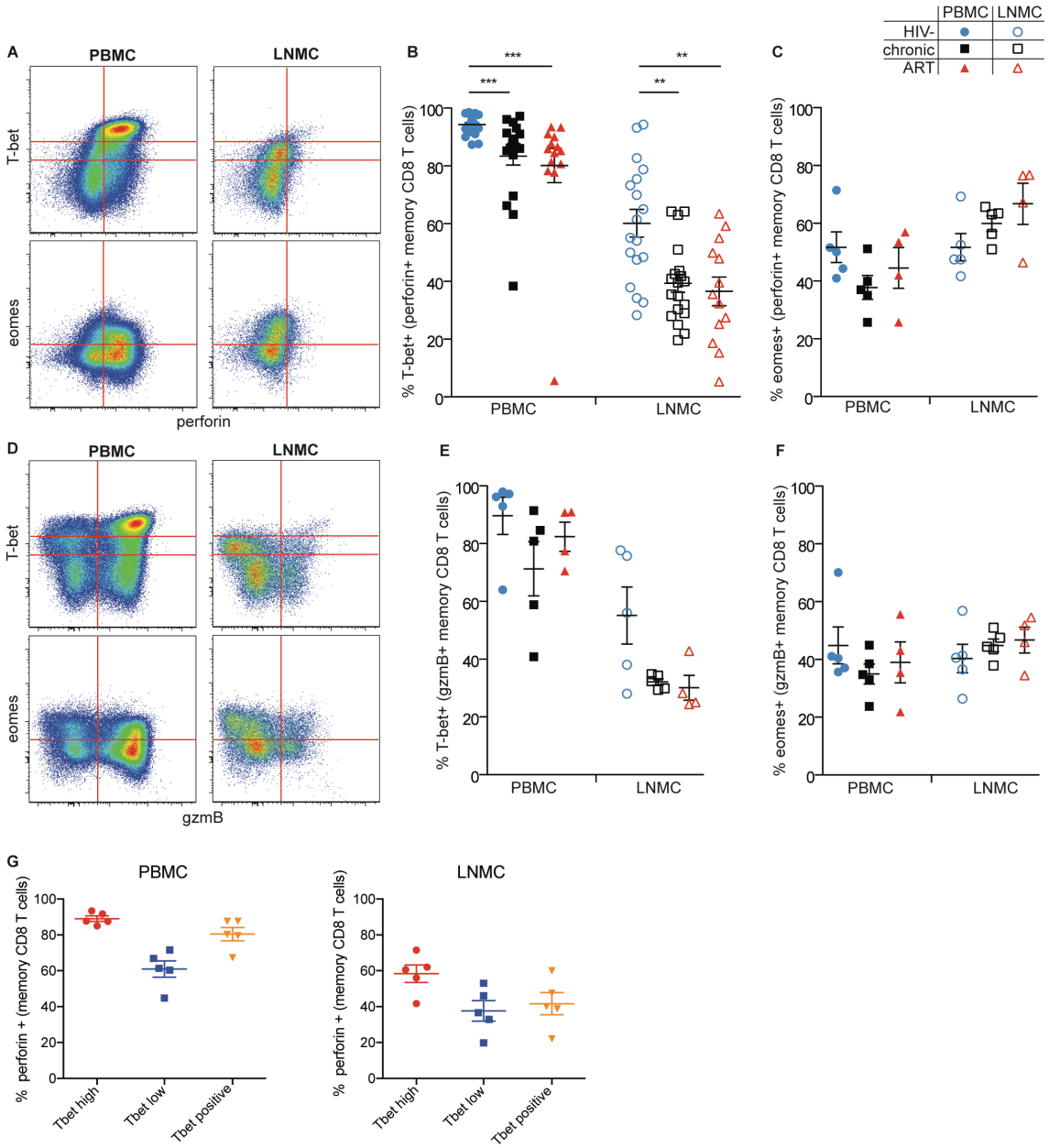

Figure S2. Cytolytic protein expression in CD8$^+$ T-cells is disconnected from classically associated transcription factors in LN. Related to Figures 2 and 3. (**A**) Representative flow cytometry plots showing memory CD8$^+$ T-cell expression of perforin vs. T-bet and eomes in PBMC and LNMC from an ART-treated HIV$^+$ individual. (**B**) Frequency of T-bet co-expression in perforin$^+$ memory CD8$^+$ T-cells in PBMC vs. LNMC. (**C**) Frequency of eomes co-expression in perforin$^+$ memory CD8$^+$ T-cells in PBMC vs. LNMC. (**D**) Representative flow cytometry plots showing memory CD8$^+$ T-cell expression of gzmB vs. T-bet and eomes in PBMC and LNMC from an ART-treated HIV$^+$ individual. (**E**) Frequency of T-bet co-expression in gzmB$^+$ memory CD8$^+$ T-cells in PBMCvs. LNMC. (**F**) Frequency of eomes co-expression in gzmB$^+$ memory CD8$^+$ T-cells in PBMC vs. LNMC. (**G**) Frequency of T-bet expressing memory CD8+ T cells that express perforin depending on the differential levels of T-bet expression. Data show five selected individuals matched PBMC and LNMC randomly selected from the sample cohort. (**B-C**, **E-F**) Statistical significance between subject groups within a tissue compartment was determined by using the Kruskal-Wallis test with Dunn's post-test. * = $P < 0.05$; ** = $P < 0.01$; *** = $P < 0.001$. HIV$^-$ (●, ○), HIV$^+$ therapy-naïve (■, □), HIV$^+$ on ART (▲, △). Ranges shown on plots represent mean +/- SEM.

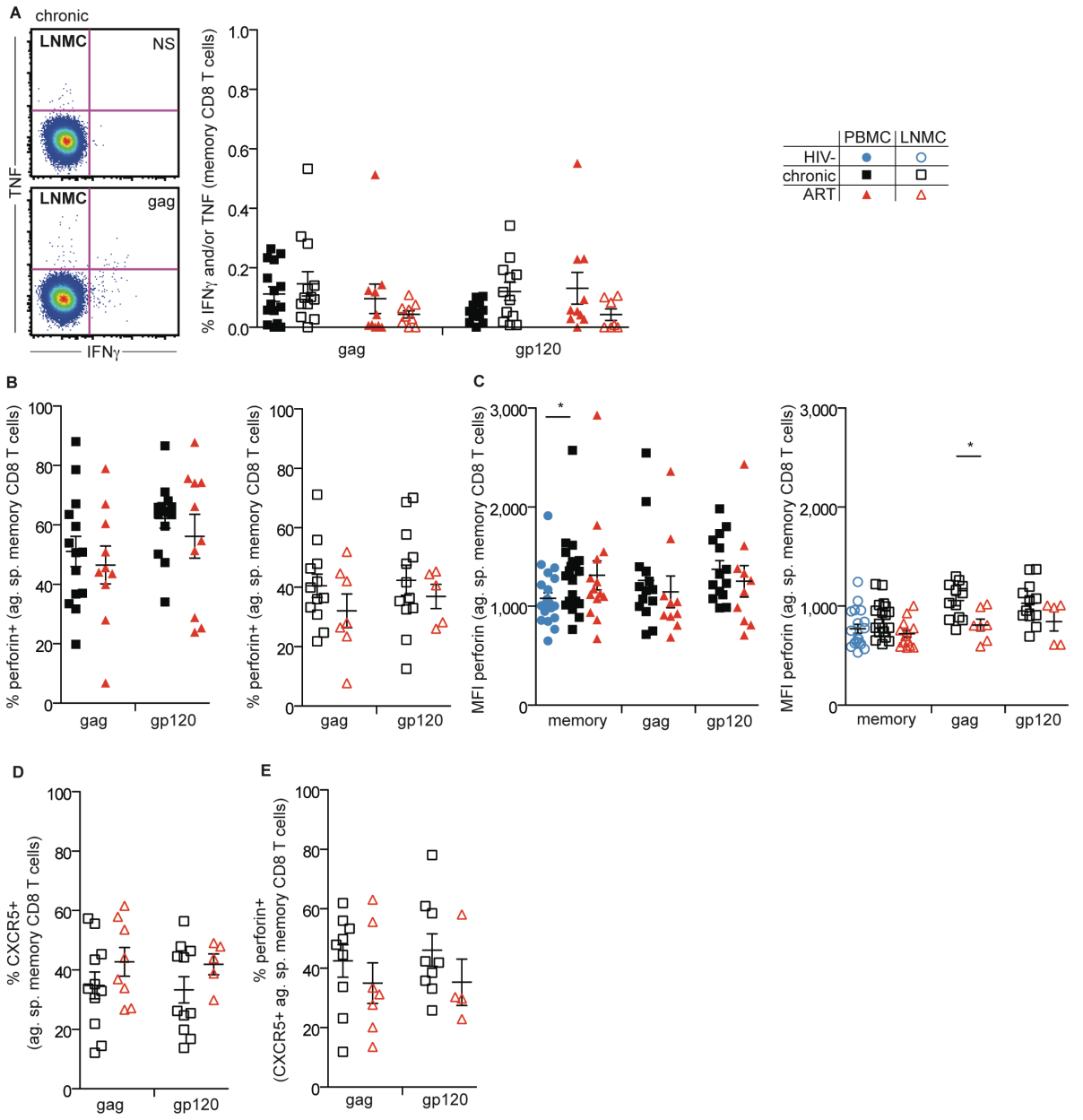

Figure S3. Expression of perforin and gzmB in HIV-specific cytokine-producing LN CD8$^+$ T-cells. Related to Figure 4. **(A)** Representative flow cytometry plots (left) showing memory CD8$^+$ T-cell production of IFNγ and/or TNF in LNMC after stimulation for 6 hours with pooled HIV clade B consensus Gag peptides (15mers overlapping by 11 amino acids). Unstimulated cells (NS) are shown to illustrate non-specific, background-level cytokine production. The graph (right) shows the frequency of Gag- and Env gp120-specific memory CD8$^+$ T-cells in PBMC vs. LNMC. Data shown are background-subtracted. **(B, C)** Perforin frequency and MFI in antigen-specific memory CD8$^+$ T-cells in PBMC vs. LNMC. Antigen-specific cells were defined on the basis IFNγ and/or TNF production in response to peptide stimulation for 6 hours. **(D)** CXCR5 frequency in antigen-specific memory CD8$^+$ T-cells in LNMC. (**E**) Perforin frequency in CXCR5$^+$ antigen-specific memory CD8$^+$ T-cells in LNMC. Statistical significance between subject groups within a tissue compartment or stimulation condition was determined by using the Kruskal-Wallis test with Dunn's post-test. Statistical significance within a subject group between tissue compartments or stimulation conditions was determined by using the Mann-Whitney two-tailed test. For both tests: * = $P < 0.05$; ** = $P < 0.01$; *** = $P < 0.001$. HIV$^-$ (●, ○), HIV$^+$ therapy-naïve (■, □), HIV$^+$ on ART (▲, △). Ranges shown on plots represent mean +/- SEM.

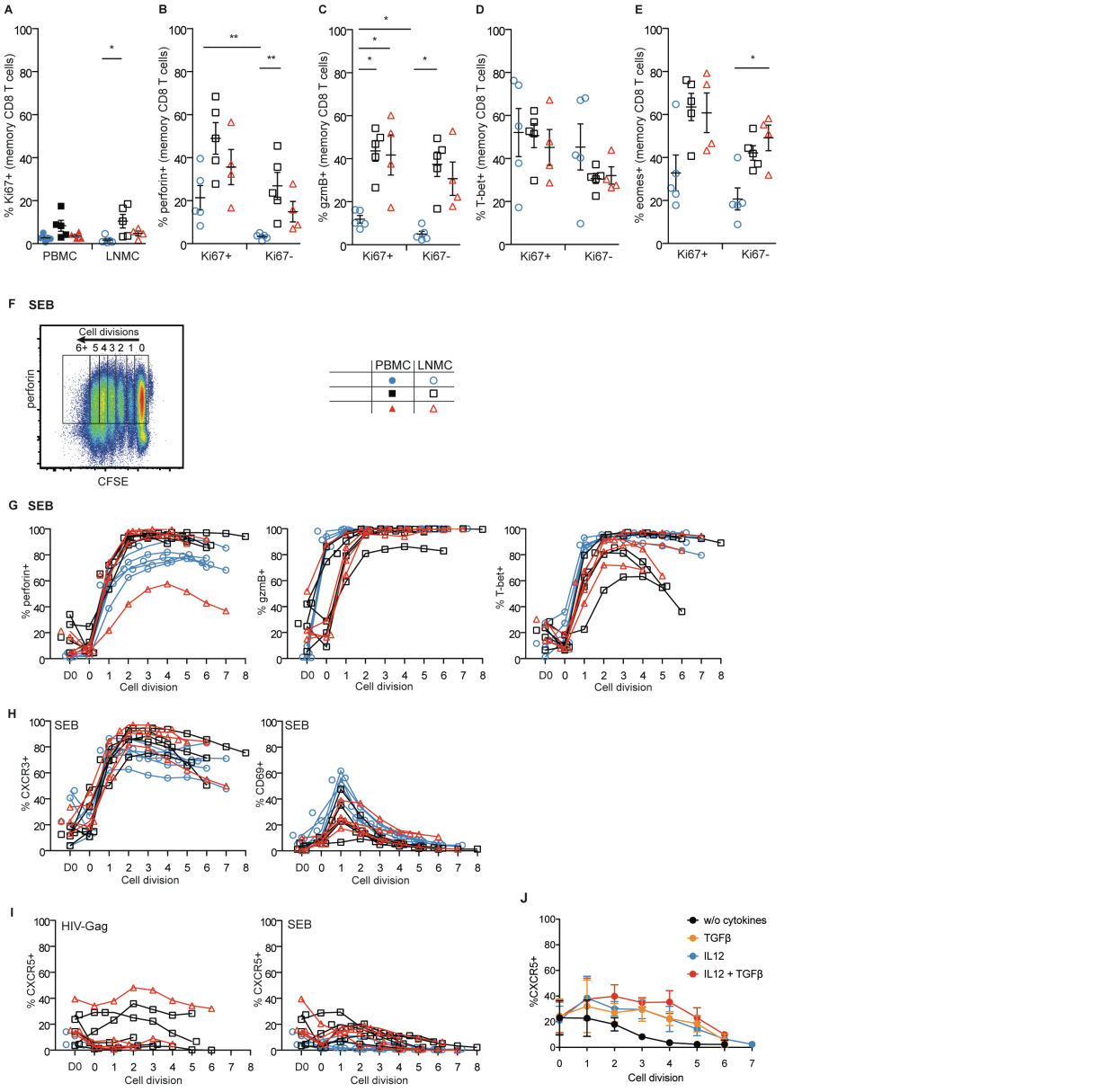

Figure S4. *Ex vivo* and *in vitro* activation of CD8$^+$ T-cells in HIV-infected subjects. Related to Figures 1 and 5 (**A**) Ki67 expression in memory CD8$^+$ T-cells in PBMC and LNMC (n=4-5). Expression of perforin (**B**), gzmB (**C**), T-bet (**D**), and eomes (**E**) in Ki67$^+$ and Ki67$^-$ memory CD8$^+$ T-cells in LNMC. Statistical significance between subject groups within an expression condition was determined by using the Kruskal-Wallis test with Dunn's post-test. Statistical significance within a subject group between expression conditions was determined by using the Mann-Whitney two-tailed test. For both tests: * = $P < 0.05$; ** = $P < 0.01$ (n=5 HIV$^-$, HIV$^+$; n=4 HIV$^+$ ART). **(F)** Representative flow cytometry plot and gating strategy to assess expression/upregulation of proteins during cell division. Perforin expression is shown for CFSE-labeled total CD8$^+$ T-cells after 5 days of stimulation with SEB. **(G, H)** Proliferating LN CD8$^+$ T-cells do not fully acquire cytolytic properties and express marker patterns associated with tissue egress. Assessment of perforin, gzmB, T-bet, CXCR3, and CD69 expression in CFSE-labeled total CD8$^+$ T-cells in LNMC after 5 days of stimulation with SEB. **(I)** Expression of CXCR5 in CFSE-labeled total CD8$^+$ T-cells in LNMC after 5 days of stimulation with either HIV clade B consensus Gag peptides (left) or SEB (right). (**J**) TGF-b and IL-12 maintain CXCR5 expression on dividing tonsil CD8+ T cells. Assessment of CXCR5 expression on CFSE-labeled tonsillar CD8$^+$ T cells after 5 days of stimulation with SEB in the presence of TGF-b and/or IL-12. Graphs show protein expression frequency vs. cell division (0 through 8 on the x-axis). D0 refers to pre-stimulation protein expression levels. HIV$^-$ (○), HIV$^+$ therapy-naïve (□), HIV$^+$ on ART (△).

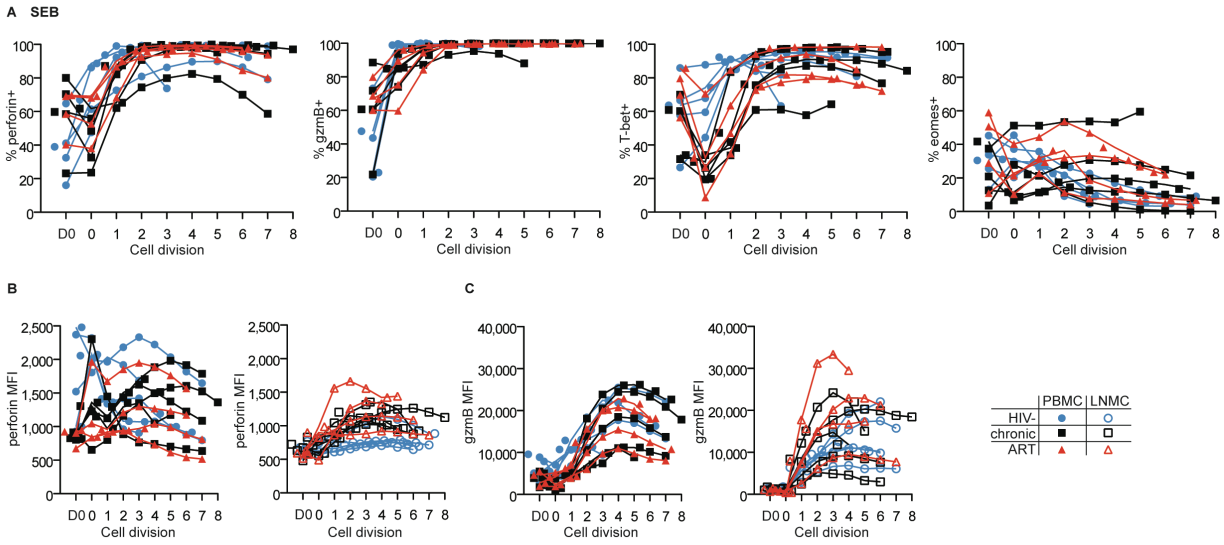

Figure S5. CD8$^+$ T-cells upregulate expression of cytolytic proteins and transcription factors after proliferation in PBMC and LNMC. Related to Figure 5. (**A**-**C**) Protein expression in CFSE-labeled total CD8$^+$ T-cells after 5 days of stimulation with SEB (*n*=5 HIV$^-$, HIV$^+$; *n*=4 HIV$^+$ ART). Graphs show protein expression frequency or MFI vs. cell division (0 through 8 on the x-axis). D0 refers to pre-stimulation protein expression levels. **(A)** Frequency of perforin, gzmB, T-bet or eomes expression in memory CD8$^+$ T-cells in PBMC. (**B**) Perforin MFI in memory CD8$^+$ T-cells in PBMC (left) and LNMC (right). (**c)** GzmB MFI in memory CD8$^+$ T-cells in PBMC (left) and LNMC (right). Graphs show protein expression frequency vs. cell division (0 through 8 on the x-axis). D0 refers to pre-stimulation protein expression levels. The gating strategy is shown in **Figure S4F**. HIV$^-$ (●, ○), HIV$^+$ therapy-naïve (■, □), HIV$^+$ on ART (▲, △).